Sebastian RÓŻOWICZ[1]

Politechnika Świętokrzyska, Katedra Elektrotechniki Przemysłowej i Automatyki

doi:10.15199/48.2018.04.43

The effect of different ignition cables on spark plug durability

***Abstract**. The article presents the effect of different types of ignition cables used in combustion engines on the wear of spark plug electrodes and the quality of exhaust gases. The research and analysis of electrode wear were conducted by electronic scanning.*

***Streszczenie.** W artykule przedstawiono wpływ różnych typów przewodów zapłonowych stosowanych w silnikach spalinowych na zużycie elektrod świec zapłonowych i jakość spalin. Badania i analizy zużycia elektrod przeprowadzono za pomocą skaningu elektronicznego. (**Wpływ różnych kabli zapłonowych na trwałość świec zapłonowych**).*

Keywords: ignition systems, spark plug, spark discharge, energy, fumes.
Słowa kluczowe: układy zapłonowe, świece zapłonowe, wyładowanie iskrowe, energia, spaliny.

Introduction

This work is a follow-up to papers [1,2] presenting the analysis of ignition systems for which the effects of spark plug electrode wear on spark discharge energy is discussed. The attempt has been made to introduce the element representing different ignition cables into ignition model.

At present air pollution is not only a local but also an international problem. At one of the international road congresses, the results of environmental pollution in 12 major European cities were presented. They showed that transport emissions amount to more than 90% of CO, 76% of hydrocarbons, 38% of NOX, more than 70% of dust and almost 100% of lead. Therefore, the analysis of combustion engine and its ignition system is highly desirable. [4].

Voltage measurement at ignition cable ends

In general, ignition systems can be divided into systems with energy storage in inductance or in capacitance [1-3].

Figure 1 presents a general diagram of a mathematical model, where R_{ls} is the spark plug and C_{45} and R_{45} denote capacity and resistance, respectively.

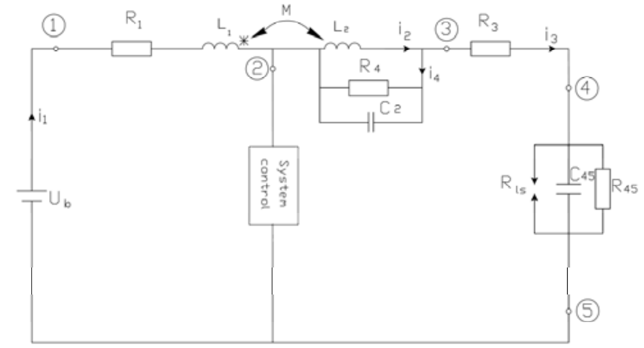

Fig. 1. Model of the ignition system for the simulation studies. U_b – battery voltage, R_1 – resistance of the ignition coil primary winding, L_1 – inductance of the ignition coil primary winding, L_2 – inductance of the ignition coil secondary winding, R_2 – resistance of the ignition coil secondary winding, R_4 – resistance representing the losses in the coil core, R_3 – radioelectrical interference resistance, R_{45} – flow resistance of the spark plug, R_{ls} – discharge resistance, C_2 – self-capacity of the coil, C_{45} – self-capacity of the spark plug, M – coupling [2]

The equivalent circuit of the ignition system presented in Fig. 1 is described by Eqs. (1) and (5) for two states of the control block. The solution to the system of equations obtained for the control block in the contact state by using the state variable method is presented as relationship (5), where it is assumed that the initial conditions, i.e. at the first switch-on, are zero.

$$
\begin{aligned}
&U_B - i_1R_1 - L_1\frac{di_1}{dt} + M\frac{di_2}{dt} = 0\\
&L_2\frac{di_2}{dt} - M\frac{di_1}{dt} + i_2R_2 + i_3R_3 + u_{C45} = 0\\
&u_{C2} = L_2\frac{di_2}{dt} - M\frac{di_1}{dt} + i_2R_2\\
&u_{C2} = i_{R4}R_4\\
&i_3 = i_2 + i_{R4} + i_{C2}\\
&i_3 = i_{R45} + i_{C45}\\
&u_{C45} = i_{R45}R_{45}\\
&i_{C2} = C_2\frac{du_{C2}}{dt}\\
&i_{C45} = C_{45}\frac{du_{C45}}{dt}
\end{aligned}
\tag{1}
$$

By introducing state variables: $x_1=i_1$, $x_2=i_2$, $x_3=u_{C2}$, $x_4=u_{C45}$ to the equation (1):

$$
\begin{aligned}
&U_B - x_1R_1 - L_1\frac{dx_1}{dt} + M\frac{dx_2}{dt} = 0\\
&L_2\frac{dx_2}{dt} - M\frac{dx_1}{dt} + x_2R_2 + R_3\frac{x_4}{R_{45}} + R_3C_{45}\frac{dx_4}{dt} + x_4 = 0\\
&x_3 = L_2\frac{dx_2}{dt} - M\frac{dx_1}{dt} + x_2R_2\\
&\frac{x_4}{R_{45}} + C_{45}\frac{dx_4}{dt} = x_2 + \frac{x_3}{R_4} + C_2\frac{dx_3}{dt}
\end{aligned}
\tag{1a}
$$

Transforming the system of equations (1), we obtain:

$$
\begin{aligned}
&\frac{dx_1}{dt} = A_1x_1 + B_1x_2 + C_1x_3 + D_1U_B\\
&\frac{dx_2}{dt} = A_2x_1 + B_2x_2 + C_2x_3 + D_2U_B\\
&\frac{dx_3}{dt} = A_3x_1 + B_3x_2 + C_3x_3 + E_3x_3 + D_3U_B\\
&\frac{dx_4}{dt} = A_4x_1 + B_4x_2 + C_4x_3 + E_4x_4 + D_4U_B
\end{aligned}
\tag{2}
$$

where the parameters are determined using the following relationships:

$$
A_1 = \frac{R_1}{\left(\frac{M^2}{L_2} - L_1\right)}\ ,\quad B_1 = \frac{MR_2}{L_2\left(\frac{M^2}{L_2} - L_1\right)}\ ,
$$

$$
C_1 = -\frac{M}{L_2\left(\frac{M^2}{L_2} - L_1\right)}\ ,\quad D_1 = -\frac{1}{\left(\frac{M^2}{L_2} - L_1\right)}
$$

$$
A_2 = \frac{-MR_1}{L_1\left(L_2 - \frac{M^2}{L_1}\right)}\ ,\quad B_2 = \frac{-R_2}{\left(L_2 - \frac{M^2}{L_1}\right)}\ ,
$$

$$
C_2=\frac{1}{\left(L_2-\frac{M^2}{L_1}\right)}\quad,\quad D_2=\frac{M}{L_1\left(L_2-\frac{M^2}{L_1}\right)}
$$

$$
\begin{aligned}
&A_3=\frac{C_{45}A_4}{C_2},\ B_3=\left(\frac{C_{45}B_4}{C_2}-\frac{1}{C_2}\right),\ C_3=\left(\frac{C_{45}C_4}{C_2}-\frac{1}{C_2}\right),\\
&D_3=\frac{C_{45}}{C_2}D_4U_B,\ E_3=\left(\frac{1}{C_2R_{45}}+\frac{C_{45}E_4}{C_2}\right)\\
&A_4=\left(\frac{MA_1}{2R_3C_{45}}-\frac{L_2A_2}{2R_3C_{45}}\right),\ B_4=\left(\frac{MB_1}{2R_3C_{45}}-\frac{L_2B_2}{2R_3C_{45}}+\frac{R_2}{2R_3C_{45}}\right),\\
&C_4=\left(\frac{MC_1}{2R_3C_{45}}-\frac{L_2C_2}{2R_3C_{45}}\right),\ D_4=\frac{-L_2D_2}{2R_3C_{45}},\ E_4=-\left(\frac{R_3}{2R_3C_{45}R_{45}}+\frac{1}{2R_3C_{45}}\right)
\end{aligned}
\tag{3}
$$

The solution to Equation (2) has the form:

$$
x=\begin{bmatrix}x_1\\x_2\\x_3\\x_4\end{bmatrix},\quad A=\begin{bmatrix}A_1 & B_1 & C_1 & 0\\ A_2 & B_2 & C_2 & 0\\ A_3 & B_3 & C_3 & E_3\\ A_4 & B_4 & C_4 & E_4\end{bmatrix},\quad B=U_B\begin{bmatrix}D_1\\D_2\\D_3\\D_4\end{bmatrix}
\tag{4}
$$

At the first switch-on, the initial conditions are zero and Eq. (4) assumes the form:

$$
\frac{d}{dt}x=Ax+B\quad,\quad x=e^{At}x_0+\int_0^t e^{A(t-\tau)}Bd\tau
$$

$$
x=\int_0^t e^{A(t-\tau)}Bd\tau
\tag{5}
$$

The solution to the system of equations obtained for the control block in the non-contact state by using the state variable method is presented as relationship (9), where the initial conditions, i.e. the final conditions from the previous state, need to be calculated from the formulae for the control block in the contact state for the time equal to the time of contact.

$$
\begin{aligned}
&U_B-i_3R_1-L_1\frac{di_3}{dt}+M\frac{di_2}{dt}-L_2\frac{di_2}{dt}+M\frac{di_3}{dt}-i_3R_3-u_{C45}=0\\
&u_{C2}=L_2\frac{di_2}{dt}-M\frac{di_3}{dt}+i_2R_2\\
&u_{C2}=i_{R4}R_4\\
&i_3=i_2+i_{R4}+i_{C2}\\
&i_3=i_{R45}+i_{C45}\\
&u_{C45}=i_{R45}R_{45}\\
&i_{C2}=C_2\frac{du_{C2}}{dt}\\
&i_{C45}=C_{45}\frac{du_{C45}}{dt}
\end{aligned}
\tag{6}
$$

In this case, the unknowns are: i_2, i_3, i_{R4}, i_{C2}, i_{R45}, i_{C45}, u_{C2}, and u_{C45}.

By introducing state variables: $x_1=i_2$, $x_2=i_3$, $x_3=u_{C2}$, $x_4=u_{C45}$ to the equation (6):

$$
\begin{aligned}
&U_B-x_2(R_1+R_3)+(M-L_1)\frac{dx_2}{dt}+(M-L_2)\frac{dx_1}{dt}-x_4=0\\
&x_3=L_2\frac{dx_1}{dt}-M\frac{dx_2}{dt}+x_1R_2\rightarrow\frac{dx_2}{dt}=\frac{L_2}{M}\frac{dx_1}{dt}+x_1\frac{R_2}{M}-\frac{1}{M}x_3\\
&x_2=x_1+\frac{x_3}{R_4}+C_2\frac{x_3}{dt}\quad\rightarrow\quad C_2\frac{x_3}{dt}=-x_1+x_2-\frac{x_3}{R_4}\\
&x_2=\frac{x_4}{R_{45}}+C_{45}\frac{dx_4}{dt}\quad\rightarrow\quad C_{45}\frac{dx_4}{dt}=x_2-\frac{x_4}{R_{45}}
\end{aligned}
\tag{6a}
$$

Transforming the system of equations (6), we obtain:

$$
\begin{aligned}
&\frac{dx_1}{dt}=a_1x_1+b_1x_2+c_1x_3+d_1x_4+e_1U_B\\
&\frac{dx_2}{dt}=a_2x_1+b_2x_2+c_2x_3+d_2x_4+e_2U_B\\
&\frac{dx_3}{dt}=a_3x_1+b_3x_2+c_3x_3\\
&\frac{dx_4}{dt}=b_4x_2+d_4x_4
\end{aligned}
\tag{7}
$$

For the system of equations (7) the parameters a_1.....d_4 are defined by the relationships:

$$
\begin{aligned}
&a_1=-\frac{R_2(M-L_1)}{[L_2(M-L_1)+M(M-L_2)]}\ ,\ b_1=\frac{M(R_1+R_3)}{[L_2(M-L_1)+M(M-L_2)]},\\
&c_1=\frac{(M-L_1)}{[L_2(M-L_1)+M(M-L_2)]}\ ,\ d_1=\frac{M}{[L_2(M-L_1)+M(M-L_2)]},\\
&e_1=-d_1\\
&a_2=\frac{a_1L_2+R_2}{M},\ b_2=\frac{b_1L_2}{M},\ c_2=\frac{c_1L_2-1}{M},\ d_2=\frac{d_1L_2}{M}\ ,\\
&e_2=-\frac{e_1L_2}{M}\quad a_3=-\frac{1}{C_2}\ ,\ b_3=\frac{1}{C_2}\ ,\ c_3=-\frac{1}{C_2R_4}\ ,\\
&b_4=\frac{1}{C_{45}}\ ,\ d_4=-\frac{1}{C_{45}R_{45}}
\end{aligned}
\tag{8}
$$

The solution to Equation (7) has the form:

$$
x=\begin{bmatrix}x_1\\x_2\\x_3\\x_4\end{bmatrix}\ ,\ A=\begin{bmatrix}a_1 & b_1 & c_1 & d_1\\ a_2 & b_2 & c_2 & d_2\\ a_3 & b_3 & c_3 & 0\\ 0 & b_4 & 0 & d_4\end{bmatrix}\ ,\ B=U_B\begin{bmatrix}e_1\\e_2\\0\\0\end{bmatrix}
\tag{9}
$$

$$
\frac{d}{dt}x=Ax+B\quad,\quad x=e^{At}x_0+\int_0^t e^{A(t-\tau)}Bd\tau
$$

x_0 – initial conditions, or final conditions from the previous state, to be calculated from the formulae for the control block in the contact state for the time equal to the time of contact.

The time *t* will be counted from the moment the block is no longer in the contact state.

Three types of ignition cables consistent with ISO 3808–02 standard were tested. A series of measurements were taken on a test stand modelling the actual arrangement of the ignition cables. In Fig. 1 the tested cables were labelled 1,2 and 3.

1) Class "F" cable of the diameter of 7mm, using double insulation (silicone) layers separated by nylon fiber reinforcement. Wire-wound reactive core using twisted resistive wire;
2) Class D cable of the diameter of 7mm, built of one insulation layer (EPDM). Carbon-acrylic core;
3) Class "E" cable, of the diameter of 7 mm, built of two silicone (insulation) layers separated by nylon fiber reinforcement. Carbon-Kevlar Core.
4) For different ignition cables, in the ignition system, the discharge energy was determined on the basis of results presented in Fig. 2 and the measurements taken on a real object. It amounts to:
5) for cable 1, class "F", 33,8mJ,
6) for cable 2, class "E", 33,1mJ
7) for cable 3, class "D", 32,6mJ
8) As can be seen the output voltage waveform differs from the response of the conductor represented by the concentrated resistance. Therefore, it is reasonable to assume that the ignition wire for short times of voltage pulses build-up can be treated as a long line.

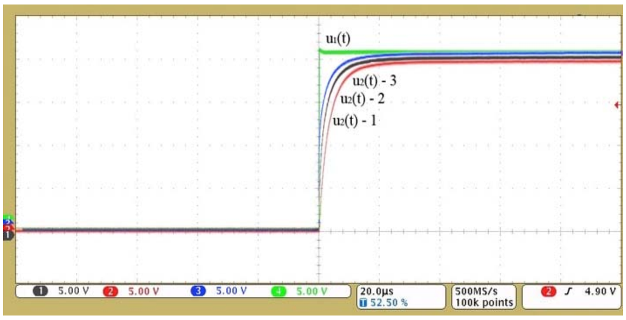

Fig.2. Voltage waveform at the end of ignition cable for unit step function input

In the next stage of the study aiming to determine the effect of the ignition cable on the voltage of spark discharge, the waveforms of the ignition coil output voltage and the voltage at the end of the ignition cable, (that is, the supply voltage for the ignition of spark plug) were recorded. The experiments were carried as shown in the diagram in Figure 3 and their results are presented in Figure 4.

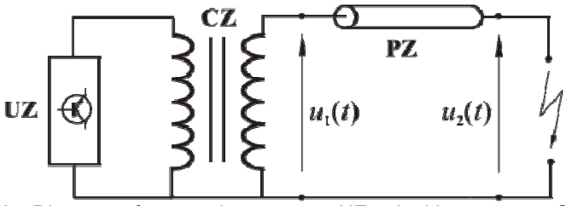

Fig.3. Diagram of measuring system: UZ – ignition system, CZ – ignition coil, PZ - ignition cable

The average results of measurements using a programmable LRC bridge at frequency f = 250 kHz are presented in Table 1.

Table 1. Measurement results of ignition cable impedance

No of cable	Impedance at idle	Impedance in short circuit
	[kΩ]	[kΩ]
1	2.200 – *j*13.040	6.079 – *j* 0.0089
2	3.880 – *j* 11.864	9.186 – *j* 0.3614
3	3.800 – *j* 12.872	8.570 – *j* 0.3229

The subsequent stage of the study included numerical experiments. Their purpose was to determine voltage at the end of ignition cable $u_2(t)$, that is, the supply voltage for the ignition of spark plug. The supply voltage is defined as follows:

$$U_2 = U_1\left(ch\gamma\, l - \frac{Z_C}{Z_0} sh\gamma\, l\right) \tag{10}$$

Wave parameters that appear in (11) are determined from the following equations:

$$Z_C = \sqrt{Z_0 Z_Z} \quad , \quad th\gamma\, l = \sqrt{\frac{Z_Z}{Z_0}} \tag{11}$$

where: Z_0 – input impedance of a long line at idle, Z_Z - input impedance of a long line in short circuit, Z_C – wave impedance of a long line, γ - propagation constant of a long line, l – the length of the line.

For the $u_1(t)$ sinusoidal voltage at the input of the line and wave parameters of the examined ignition cables calculated on the basis of measurement results from Table 1, the voltage waveforms at the end of the line were obtained. They are presented in Fig. 4. It is easy to notice that $u_2(t)$ voltage was shifted in phase relative to $u_1(t)$ and decreased the amplitude.

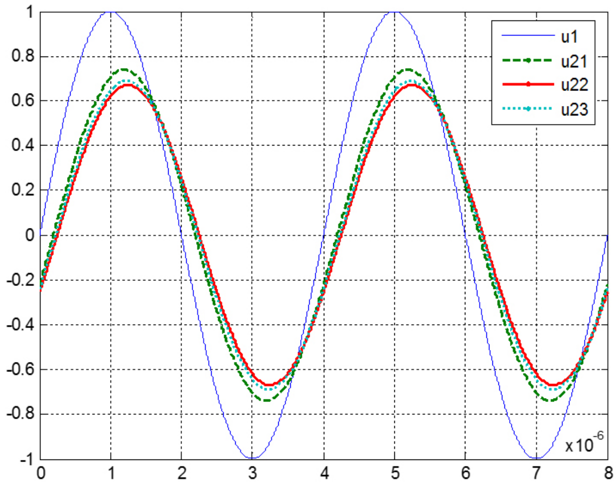

Fig. 4. Simulation results for different ignition cables

On the basis of simulation results it can be concluded that the approximation of ignition cable by means of a long line gives positive results. A time shift of $u_2(t)$ voltage and the change of its amplitude are observed.

The effect of the ignition cable on the operation of spark plug

The investigations performed under real operating conditions involved observing the microscopic gap between the spark plug electrodes before the tests and after every 500 hours of operation. The tests were carried out using a purpose-built setup presented in Fig.5.

Fig.5. A setup to test ignition systems.

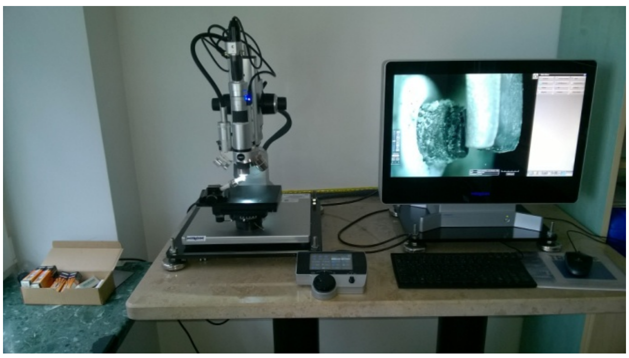

Fig 6. Microscope stand for the observation of electrode wear

Figure 6 shows the digital microscope produced by a Japanese company HIROX, model KH-8700. The device has the magnification of 35 to 5000. It enables us to measure geometrical quantities as well as images of the profiles of the examined surface.

The operational tests were performed for the systems with cables 1, 2 and 3 in the same, defined operational conditions. The analysis of spark plug wear was conducted by electronic scanning. Case examples of spark plug wear are presented in Fig.7.

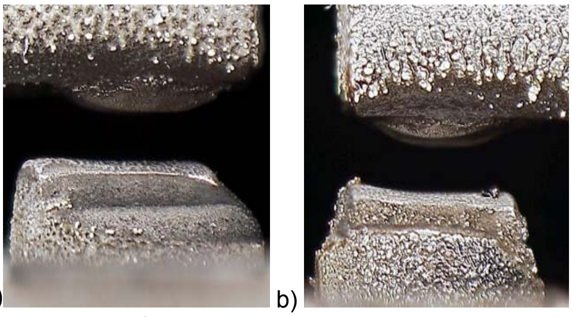

a) b)

Fig. 7. The image of the gap between electrodes
a) spark plug working with F class cable of the diameter of 7 mm using double insulation (silicone) layers with wire-wound reactive core using twisted resistive wire;
b) spark plug working with D class cable of the diameter of 7 mm made of insulation layer (EPDM mixture) with carbon- acrylic core (visible electrode erosion and a significant carbon deposit may indicate non-optimal composition of exhaust gases).

The photographs presented in the next part of the paper show some results of the experiments on the wear of spark plug electrodes after a 500-hour operation. The experiments are continued for temperature changes.

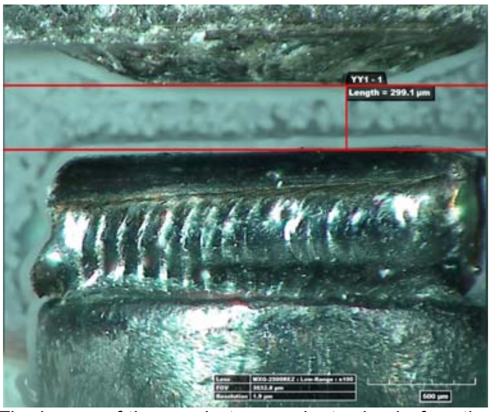

Fig .8. The image of the gap between electrodes before the test

Fig.9. The image of the gap between electrodes after a 500-hour operation of the ignition system with a high voltage cable of F class.

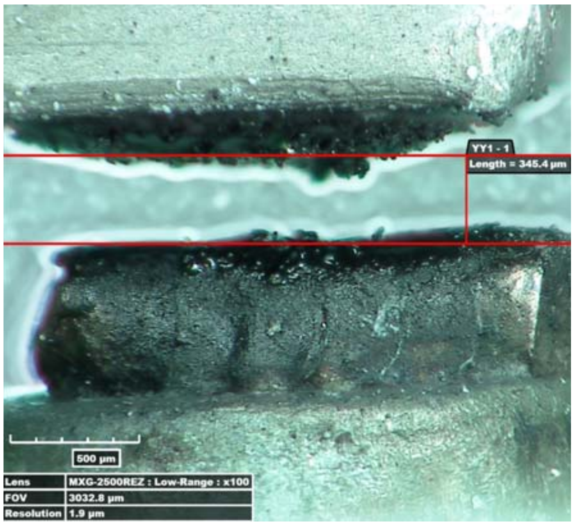

Fig.10. The image of the gap between electrodes after a 500-hour operation of the ignition system with high voltage cable of D class.
.

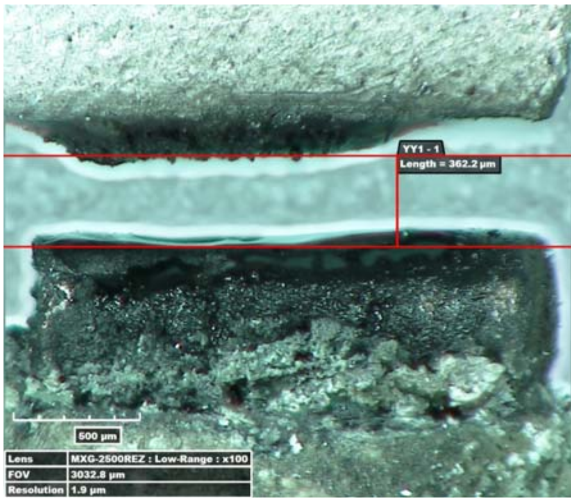

Fig.11. The image of the gap between electrodes after a 500-hour operation of the ignition system with high voltage cable of E class.

Conclusion

The research on the ignition system for three types of ignition cables indicates that the type of the cable has considerable influence on the value of spark discharge energy, the electrode burnout and the composition of exhaust gases.

Laboratory tests allow for the verification of computer simulations. They show that the value of electric discharge energy depends on both the quality of fuel delivered to the combustion chamber and the wear of the spark plug electrodes. It should also be noted that the wear of spark plug electrodes significantly affects the value of electric discharge.

As can be seen the value of spark discharge has a major impact on the wear of the spark plug electrodes.

The results suggest that if pressure in the combustion chamber is also considered some interesting conclusions concerning its influence on spark discharge energy can be drawn and investigated. The authors think that the novelty of this paper is the possibility (based on experimental results) to select such R and C of spark plug that allows the mathematical modelling of its wear using the proposed model (without necessity to conduct the experiment).

***Author**: dr inż. Sebastian Różowicz, Politechnika Świętokrzyska, Katedra Elektrotechniki Przemysłowej i Automatyki, Aleja. Tysiąclecia Państwa Polskiego 7, 25-314 Kielce, E-mail: s.rozowicz@tu.kielce.pl*

REFERENCES

[1] S. Różowicz Sz. Tofil "The influence of impurities on the operation of selected fuel ignition systems in combustion engines" ISTET 2015.
[2] S. Różowicz " The effect of parameter change of ignition system primary side R,L and C elements on the value of spark discharge energy" (in Polish) Przegląd Elektrotechniczny" ISSN 0033-2097, R. 92 NR 5/2016.
[3] S. Bolkowski, " Theory of Electrical Circuits" (in Polish)", WNT 2012.
[4] P. Kubiak, M. Zalewski: " Diagnostic Workshop of Motor Vehicles" (in Polish). WKŁ 2012
[5]N. Radek, Determining the operational properties of steel beaters after electrospark deposition. Eksploatacja i Niezawodność – Maintenance and Reliability 4, 10-16, (2009).
[6] N. Radek, K. Bartkowiak, Performance properties of electro-spark deposited carbide-ceramic coatings modified by laser beam. Physics Procedia (Elsevier) 5, 417-423 (2010).
[7] W. Danilczyk, St. Kruczyński, M. Stępniewski, R. Wołoszyn, Evaluation of Pt-NiCr connections on spark plug electrodes. VII International Scientific and Technical Conference "Logistics, transport systems, transport safety" (in Polish) – LOGITRANS 2010, Szczyrk.
[8] A. Zawadzki, S. Różowicz, Application of input – state of the system transformation for linearization of some nonlinear generators, International Journal of Control, Automation and Systems (2015) 13(3):1-8 ; DOI 10.1007/s12555-014-0026-3.
[9] Różowicz S.: Analysis of the effect of the ignition system construction and parameters on the value of the discharge energy, PhD dissertation (in Polish), PŚK 2012,
[10] Stone C, Brown A, Beckwith P. Cycle-by-cycle variations in spark ignition engine combustion – part II: modeling of flame kernel displacements as a cause of cycle-by-cycle variations. SAE paper 960613; 1996.
[11] Robinet C, Andrzejewski J, Higelin P. Cycle-to-cycle variation study of an si engine fired by spark plug and a non-conventional device. SAE paper 972986; 1997.
[12] Hunicz J., Wac E., Kabała J., Comparative study of new spark plug designs, operation and reliability. Operation and Reliability (in Polish) 3/2006
[13] Herweg R, Ziegler GFW. Flame kernel formation in a sparkignition engine. In: International sym-posium COMODIA 90; 1990. p. 173–8.
[14] Lee K, Kim K. Influence of initial combustion in SI engine on following combustion stage and cycle-by-cycle variations in combustion process. Int J Automot Technol 2001;2(1):25–31.
[15] Lee Y, Boehler J. Flame kernel development and its effects on engine performance with various spark plug electrode configurations. SAE paper 2005-01-1133; 2005.
[16] Osamura H. Development of long life and high ignitability iridium spark plug. In: Seoul 2000 FISI-TA world automotive congress, Paper number F2000A144, Korea; 2000.